
PATH DEVELOPMENT NETWORK WITH FINITE-DIMENSIONAL LIE GROUP REPRESENTATION

A PREPRINT

 **Hang Lou**

Department of Mathematics
University College London
hang.lou.19@ucl.ac.uk

 **Siran Li**

Department of Mathematics
Shanghai Jiao Tong University
s14025@nyu.edu

 **Hao Ni**

Department of Mathematics
University College London
h.ni@ucl.ac.uk

April 5, 2022

ABSTRACT

The path signature, a mathematically principled and universal feature of sequential data, leads to a performance boost of deep learning-based models in various sequential data tasks as a complimentary feature. However, it suffers from the curse of dimensionality when the path dimension is high. To tackle this problem, we propose a novel, trainable path development layer, which exploits representations of sequential data with the help of finite-dimensional matrix Lie groups. We also design the backpropagation algorithm of the development layer via an optimisation method on manifolds known as trivialisation. Numerical experiments demonstrate that the path development consistently and significantly outperforms, in terms of accuracy and dimensionality, signature features on several empirical datasets. Moreover, stacking the LSTM with the development layer with a suitable matrix Lie group is empirically proven to alleviate the gradient issues of LSTMs and the resulting hybrid model achieves the state-of-the-art performance.

Keywords Path development · Lie group · Time series modelling · Path signature · Recurrent neural network · Rough path theory

1 Introduction

Signature-based methods are an emerging technology for the modelling of time series data. The signature of a path, originated from rough path theory in stochastic analysis (Lyons et al. [2007]), has shown its promise as an efficient feature representation of time series data, which can be combined with suitable machine learning models (*e.g.*, deep learning and tree-based models) to further boost prediction performance (Xie et al. [2017], Arribas et al. [2018], Morrill et al. [2019]).

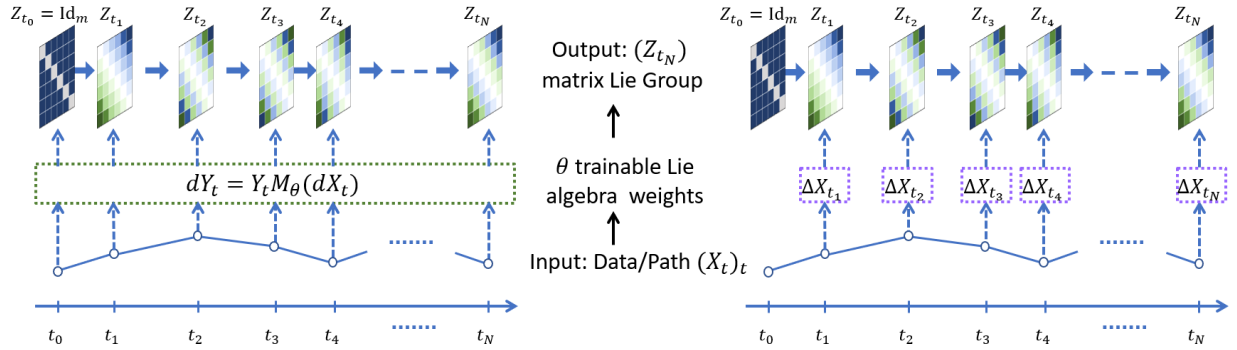
The signature of a path $X : [0, T] \rightarrow \mathbb{R}^d$, in heuristic terms, is a series of non-commutative monomials which provides a top-down description of X in terms of its effects on non-linear systems (Lyons [2014]):

$$\left(1, \mathbf{X}_{[0,T]}^{(1)}, \dots, \mathbf{X}_{[0,T]}^{(k)}, \dots\right),$$

where $\mathbf{X}_{[0,T]}^k = \int_{0 < t_1 < \dots < t_k < T} dX_{t_1} \otimes \dots \otimes dX_{t_k} \in \mathbb{R}^{d \times k}$.

In contrast to deep learning based models that are computationally expensive and difficult to interpret in the large, the signature of time series is a mathematically principled feature representation, which has been proven to be universal and enjoy desirable analytic-geometric properties. The signature transformation can be used as a deterministic and pluggable layer in neural networks (Kidger et al. [2019]). In practice, nevertheless, the signature transformation faces three major challenges: (1), the curse of dimensionality — the dimension $\left(\sum_{i=0}^k d^i = \frac{d^{k+1}-1}{d-1}\right)$ of the truncated signature up to the k^{th} term grows geometrically in the path dimension d ; (2), it is not data-adaptive, hence may be ineffective in certain learning tasks; and, (3) it incurs potential information loss due to finite truncation of the signature feature.

Figure 1: We give a high level summary of the proposed development layer with the output and trainable weights taking values in the matrix Lie group G and the corresponding Lie algebra \mathfrak{g} , respectively. (Left) It can be interpreted as a solution to the linear controlled differential equation driven by a driving path (Definition 2.2), which is a continuous lift of sequential data. (Right) It can be viewed as an analogy of the RNNs, but with a simpler form (Eq. (2)).



To address those issues, we propose an alternative trainable feature representation of time series based on the *development* of a path *à la* Cartan (Driver [1995]). It is an important mathematical tool in rough path theory to study signature inversion (Lyons and Xu [2017]) and the uniqueness of expected signature (Boedihardjo and Geng [2020], Hambly and Lyons [2010], Chevyrev and Lyons [2016]). The path development of X is a function from $L(\mathbb{R}^d, \mathfrak{g})$ to G as follows:

$$M \mapsto \sum_{k \geq 0} \left\{ \int_{0 < t_1 < \dots < t_k < T} \prod_{j=1}^k M(dX_{t_j}) \right\}. \quad (1)$$

Here \mathfrak{g} is a Lie algebra and G is its corresponding Lie group, which shall be suitably chosen in context; $L(\mathbb{R}^d, \mathfrak{g})$ is the vector space of linear transforms from \mathbb{R}^d to \mathfrak{g} . Recall that a key algebraic structure in the definition of path signature is tensor product, which is non-commutative in nature. Here, for path development, non-commutativity also plays a central role, as is reflected in the matrix multiplication on the right-hand side of Eq. (1).

The development preserves various favourable geometric and analytic properties of the path X , hence is promising to serve as a good feature representation of sequential data. It is shown in Chevyrev and Lyons [2016] that, for suitably chosen Lie algebra \mathfrak{g} , the path development constitutes *universal and characteristic* features, which is the same with the path signature. But the development takes values in matrix groups of finite dimensions (independent of the path dimension), while the path signature is ∞ -dimensional.

Motivated by this, we construct what we term as the *path development layer*, which transforms any sequential data $x = (x_0, \dots, x_N) \in \mathbb{R}^{d \times (N+1)}$ to its path development $z = (z_0, \dots, z_N) \in G^{N+1}$ under a trainable linear map $M_\theta: \mathbb{R}^d \rightarrow \mathfrak{g}$. For each $n \in \{0, \dots, N\}$ we set

$$z_{n+1} := z_n \exp(M_\theta(x_{n+1} - x_n)), \quad z_0 = \text{Id}_m, \quad (2)$$

where θ is the model parameter, Id_m is the identity matrix, and \exp is the matrix exponential. It has a recurrence structure analogous to that of the RNNs.

To optimise model parameters in the development layer, we exploit the recurrence structure (2) and the Lie group structure of the range of the output to design an efficient gradient-based optimisation method. This is achieved via combining the backpropagation through time of the RNNs and an optimisation method on manifolds known as “trivialisation”; see Lezcano-Casado [2019]. In particular, when choosing the Lie algebra of the orthogonal group, the algebraic structure of the development output helps establish the boundedness of gradient. This alleviates the gradient vanishing/exploding problems of the backpropagation through time, thus leading to a more stable training process. To the best of our knowledge, this work is the first of the kind to (1), construct a trainable layer based on path development; and (2), design the backpropagation of the development layer, taking into account adequate Lie group structures.

Key advantages of the proposed path development layer include the following: (1), it provides mathematically principled features, which are characteristic and universal; (2), it is a data-adaptive, trainable layer that can be plugged into general neural network architectures; (3) it is applicable to high-dimensional time series; and (4), it helps stabilise the training process. Numerical results validate the efficacy of the development layer in comparison to the signature layer and several other continuous models. Moreover, the hybrid model obtained by stacking together LSTM with the

development layer consistently achieves outstanding accuracy performance with more stable training processes and less need for hyper-parameter tuning. We also provide a toy example of N -body simulation, which demonstrates that the inherited equivariance of the learning task can be effectively incorporated into the development model by properly choosing the Lie group G , thus leading to performance boost. This may offer a novel, promising class of models based on the development module for trajectories of moving data clouds.

1.1 Related Work

1.1.1 Recurrent Neural Networks

Recurrent Neural Network (RNN) and its variants are popular models for sequential data, which achieve superior empirical performance on various time series tasks Hochreiter and Schmidhuber [1997], Cho et al. [2014], Bai et al. [2018]. It enjoys excellent capacity for exhibiting temporal dynamic behaviour due to the recurrence structure of hidden states; however, RNN-type models may encounter difficulty in capturing long-term temporal dependency and are prone to problems of vanishing/exploding gradients Bengio et al. [1994]. It has been demonstrated Arjovsky et al. [2016], Lezcano-Casado [2019] that restricting weight matrices of RNN to the unitary group proves helpful for handling the issues above and stabilising the training processes. Our proposed development layer has recurrence structures similar to those of the RNNs (2), but in a much simpler and more explicit form. Furthermore, our development has its outputs constrained to matrix Lie group, which has positive effects on stability and long-term temporal dependency of training processes.

1.1.2 Continuous time series modelling

Continuous time series models have recently attracted increasing attention due to their strength on treating irregular time series in a unified fashion. Popular models inspired by differential equations include Neural ODEs (Chen et al. [2018]), Neural SDEs (Liu et al. [2019]), and Neural controlled differential equations (Kidger et al. [2020], Morrill et al. [2021]). The model based on path signature and development we propose here, similar in spirit to the above models, takes a continuous perspective — it embeds discrete time series to the path space and solves for linear controlled differential equations driven by the path. It has shown advantages in coping with time series which are irregularly sampled, of variable length, or invariant under time reparameterisation.

2 Preliminaries

2.1 Path Signature

We present here a self-contained, brief summary of the path signature, which can be used as a principled and efficient feature of time series data. See Lyons et al. [2007], Levin et al. [2013], Chevyrev and Kormilitzin [2016], Kidger et al. [2019] and many other references.

Denote by $\mathcal{V}_1([0, T], \mathbb{R}^d)$ the space of continuous paths $[0, T] \rightarrow \mathbb{R}^d$ with finite length, and by $T((\mathbb{R}^d))$ the tensor algebra space:

$$T((\mathbb{R}^d)) := \bigoplus_{k \geq 0} (\mathbb{R}^d)^{\otimes k}.$$

$T((\mathbb{R}^d))$ becomes an algebra when equipped with tensor product and component-wise addition. The signature takes values in $T((\mathbb{R}^d))$, and its zeroth component is always 1.

Definition 2.1 (Path Signature). Let $J \subset [0, T]$ be a bounded interval and $X \in \mathcal{V}_1([0, T], \mathbb{R}^d)$. The signature of X over J , denoted as $S(X)_J$, is given by

$$S(X)_J = (1, \mathbf{X}_J^1, \mathbf{X}_J^2, \dots),$$

where $\mathbf{X}_J^k = \int_{\substack{u_1 < \dots < u_k \\ u_1, \dots, u_k \in J}} dX_{u_1} \otimes \dots \otimes dX_{u_k}$ for each $k \geq 1$.

The truncated signature of X of order k is

$$\pi_k(S(X))_J \equiv S^k(X)_J := (1, \mathbf{X}_J^1, \mathbf{X}_J^2, \dots, \mathbf{X}_J^k). \quad (3)$$

Its dimension equals $\sum_{i=0}^k d^i = \frac{d^{k+1}-1}{d-1}$, which grows exponentially in k . The range of signature of all paths in $\mathcal{V}_1([0, T], \mathbb{R}^d)$ is denoted as $S(\mathcal{V}_1([0, T], \mathbb{R}^d))$.

The signature can be deemed as a non-commutative version of the exponential map defined on the space of paths. Indeed, consider $\exp : \mathbb{R} \rightarrow \mathbb{R}$, $\exp(t) = e^t = \sum_{k=0}^{\infty} \frac{t^k}{k!}$; it is the unique C^1 -solution to the linear differential equation $d\exp(t) = \exp(t)dt$. Analogously, the signature map $t \mapsto S(X_{0,t})$ solves the following linear differential equation:

$$\begin{cases} dS(X)_{0,t} = S(X)_{0,t} \otimes dX_t, \\ S(X)_{0,0} = \mathbf{1} := (1, 0, 0, \dots). \end{cases} \quad (4)$$

2.2 Path Development on matrix Lie group

Let G be a finite-dimensional Lie group with Lie algebra \mathfrak{g} . For concreteness, we assume that \mathfrak{g} is a matrix Lie algebra throughout this paper (see Ado's theorem). Examples of commonly used matrix Lie algebras include:

$$\begin{aligned} \mathfrak{gl}(m; \mathbb{F}) &:= \{m \times m \text{ matrices over } \mathbb{F}\} \cong \mathbb{F}^{m \times m} \ (\mathbb{F} = \mathbb{R} \text{ or } \mathbb{C}), \\ \mathfrak{so}(m, \mathbb{R}) = \mathfrak{o}(m, \mathbb{R}) &:= \{A \in \mathfrak{gl}(m; \mathbb{R}) : A^\top + A = 0\}, \\ \mathfrak{sp}(2m, \mathbb{R}) &:= \{A \in \mathfrak{gl}(2m; \mathbb{R}) : A^\top J_m + J_m A = 0\}, \\ \mathfrak{su}(m, \mathbb{C}) &:= \{A \in \mathfrak{gl}(m; \mathbb{C}) : \text{tr}(A) = 0, A^* + A = 0\}. \end{aligned}$$

Here and hereafter, $J_m := \begin{pmatrix} 0 & I_m \\ I_m & 0 \end{pmatrix}$; \mathfrak{g} is said to be a matrix Lie algebra if it is a Lie subalgebra of $W \equiv \mathfrak{gl}(m; \mathbb{F})$.

Definition 2.2 (Path Development). Let $M : \mathbb{R}^d \rightarrow \mathfrak{g} \subset W$ be a linear map and let $X \in \mathcal{V}_1([0, T], \mathbb{R}^d)$. The path development (*a.k.a.* ‘‘the Cartan development’’) of X on G under M is the solution Z_t to the differential equation

$$dZ_t = Z_t \cdot M(dX_t) \quad \text{for all } t \in [0, T] \text{ with } Z_0 = e, \quad (5)$$

where $e \in G$ is the group identity and \cdot denotes matrix multiplication. We write $D_M(X)$ for the endpoint of path development Z_T of X under M .

Example 2.3. For linear path $X \in \mathcal{V}_1([0, T], \mathbb{R}^d)$ and matrix Lie algebra \mathfrak{g} , the development of X on G under M is

$$D_M(X)_{0,t} = \exp(M(X_t - X_0)),$$

where $M \in L(\mathbb{R}^d, \mathfrak{g})$. (Here and hereafter, $L(V_1, V_2)$ denotes the space of linear maps $V_1 \rightarrow V_2$.) Indeed, $t \mapsto \exp(M(X_t - X_0))$ is the unique solution to (5).

In what follows, let us summarise several important properties of the path development directly related to applications in machine learning. See Lyons and Xu [2017], Boedihardjo et al. [2021] for more about path development. The proofs of Lemma 2.6 and Lemma 2.7 will be provided in Appendix A.

Lemma 2.4 (Multiplicative property of path development). *Let $X \in \mathcal{V}_1([0, s], \mathbb{R}^d)$ and $Y \in \mathcal{V}_1([s, t], \mathbb{R}^d)$. Denote by $X * Y$ the concatenation of X and Y , namely that*

$$X * Y(v) = \begin{cases} X(v) & \text{if } 0 \leq v \leq s, \\ Y(v) - Y(s) + X(s) & \text{if } s \leq v \leq t. \end{cases}$$

*Then $D_M(X * Y) = D_M(X)D_M(Y)$ for all $M \in L(\mathbb{R}^d, \mathfrak{g})$.*

Lemma 2.4 and Example 2.3 allow us to compute analytically the development of any piecewise linear path.

Example 2.5 (Hyperbolic Development). Let $X : [0, T] \rightarrow \mathbb{R}^2$ be a 2-dimensional piecewise linear path. Consider

$M : \mathbb{R}^2 \ni (x, y) \mapsto \begin{pmatrix} 0 & 0 & x \\ 0 & 0 & y \\ x & y & 0 \end{pmatrix} \in \mathfrak{so}(2, 1)$ and set $o = (0, 0, 1)^T$. Then $t \mapsto D_M(X)_{0,t}o$ is a path in the hyperboloid

$$\mathbb{H}^2 := \{x \in \mathbb{R}^3 : (x_1)^2 + (x_2)^2 - (x_3)^2 = -1, x_3 > 0\}.$$

It is known as the *hyperbolic development* of X . Here $\mathfrak{so}(2, 1)$ is the Lie algebra of the group of orientation-preserving isometries of \mathbb{H}^2 . Figure 2 visualises the evolution of the hyperbolic development.

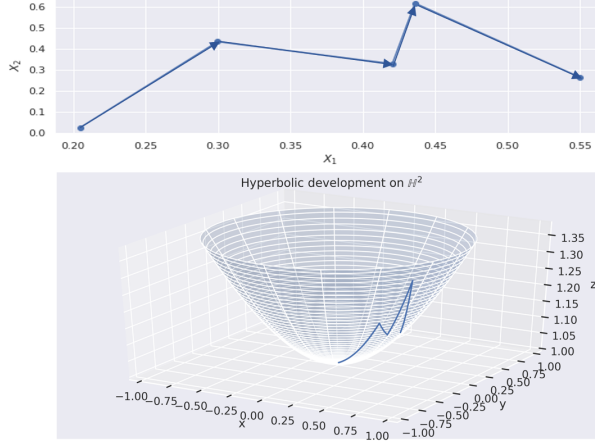


Figure 2: Upper panel: X , a 2D piecewise linear path; Lower panel: the hyperbolic development $D_M(X)$ of X .

When $M \in L(\mathbb{R}^d, W)$, there is a canonical extension $\widetilde{M} \in L(T(\mathbb{R}^d), W)$ of M , given by

$$\widetilde{M}(e_{i_1} \otimes e_{i_2} \cdots \otimes e_{i_k}) := M(e_{i_1})M(e_{i_2}) \cdots M(e_{i_k}).$$

Lemma 2.6 (Link with signature). *Let $X \in \mathcal{V}_1([0, T], \mathbb{R}^d)$ and let $M \in L(V, \mathfrak{g})$. Then $D_M(X) = \widetilde{M}(S(X))$.*

Roughly speaking, the development of a path can be thought of as $M \mapsto \sum_{k \geq 0} \widetilde{M}(\pi_k(S(X)))$, which takes the form of a generating function $L(V, W) \rightarrow W$.

Lemma 2.7 (Invariance under time-reparametrisation). *Let $X \in \mathcal{V}_1([0, T], \mathbb{R}^d)$ and let λ be a non-decreasing function from $[0, T]$ onto $[0, S]$. Define $X_t^\lambda := X_{\lambda_t}$ for $t \in [0, T]$. Then, for all $M \in L(\mathbb{R}^d, \mathfrak{g})$ and for every $s, t \in [0, T]$, $D_M(X_{\lambda_s, \lambda_t}) = D_M(X_{s, t}^\lambda)$.*

Remark 2.8. Lemma 2.7 states that the path development is invariant under time reparameterisation. The same property also holds for the path signature. Thus, the development feature removes the redundancy caused by the speed of traversing the path, hence bringing about massive dimensionality reduction and robustness in various tasks, e.g., online handwritten character recognition and human action recognition. (When the speed information is relevant to the prediction task, one may simply add the time dimension to the input data.)

When choosing adequate Lie algebras, the space of path developments constitutes a rich model space to approximate continuous functionals on the signature space.

Theorem 2.9 (Characteristic property of path development, Theorem 4.8 in Chevyrev and Lyons [2016]). *Let $x = (x_0, x_1, \dots) \in T(\mathbb{R}^d)$ such that $x^k \neq 0$ for some $k \geq 0$. For any $m \geq \max\{2, k/3\}$, there exists $M \in L(\mathbb{R}^d, \mathfrak{sp}(m, \mathbb{C}))$ such that $\widetilde{M}(x) \neq 0$. In particular,*

$$D_{\mathfrak{sp}}(S(\mathcal{V}([0, T], \mathbb{R}^d))) := \bigcup_{m=1}^{\infty} \left\{ \widetilde{M} : M \in L(\mathbb{R}^d, \mathfrak{sp}(m, \mathbb{C})) \right\}$$

separates points over $S(\mathcal{V}_1([0, T], \mathbb{R}^d))$.

Remark 2.10. Theorem 2.9 shows that if two signatures differ at a certain k^{th} level, one can find $\widetilde{M} : T(\mathbb{R}^d) \rightarrow G$ that separates the two signatures, whose resulting development has dimension at most $(\max(2, \frac{k}{3}))^2$. This number is typically much smaller than the dimension of the truncated signature up to degree k , namely $\frac{d^{k+1}-1}{d-1}$.

Meanwhile, Chevyrev and Lyons [2016] proves that the unitary representation of path development is universal to approximate continuous functionals on the signature space. See Theorem A.4 in the appendix.

2.3 Optimisation on Lie Group

In this subsection, we collect some background materials on trivialisation, a gradient-based optimisation method on Riemannian manifolds introduced in Lezcano-Casado [2019], Lezcano-Casado and Martinez-Rubio [2019]. In this work we shall focus on matrix Lie groups; see Lezcano-Casado [2019] for general manifolds.

Definition 2.11 (Trivialisation). Let G be a matrix Lie group. A surjection $\phi : \mathbb{R}^d \rightarrow G$ is called a trivialisation.

Trivialisations allow us to reduce an optimisation problem constrained on a manifold to an unconstrained problem, namely that

$$\min_{x \in G} f(x) \iff \min_{a \in \mathbb{R}^d} f(\phi(a)).$$

The right-hand side can be solved numerically by gradient descent once we have $\nabla(f \circ \phi)$ computed.

For a compact connected matrix group G with Lie algebra \mathfrak{g} , the matrix exponential \exp serves as the the ‘‘canonical’’ trivialisation. For the noncompact case where \exp is not surjective, \exp can be used as a trivialisation only locally; see Theorem 4.7 in Lezcano-Casado [2019].

Proposition 2.12 below, together with Lemma 2.13, enables a fast numerical implementation of the gradient $\nabla(f \circ \exp)$ over matrix Lie groups.

Proposition 2.12 (Gradient of the matrix exponential; Lezcano-Casado [2019]). *Let $f : \mathfrak{gl}(n; \mathbb{C}) \rightarrow \mathbb{R}$ be a scalar function and \exp be the matrix exponential. Then*

$$\nabla(f \circ \exp)(A) = (\mathrm{d}\exp)_{A^\top}(\nabla f(\exp(A))).$$

Lemma 2.13 (Rossmann [2002]). *The differential of the matrix exponential at any $A \in \mathfrak{gl}(n, \mathbb{C})$ is given by*

$$(\mathrm{d}\exp)_A(X) = \sum_{n=0}^{\infty} \frac{(-\mathrm{ad}(A))^k}{(k+1)!} (\exp(A)X),$$

where ad is the adjoint action $\mathrm{ad}(X)Y := XY - YX$.

3 Path Development Layer

3.1 Network architecture

We propose in this work a novel neural network, termed as the *path development layer*, as a general and trainable module on time series data.

In practice, one often observes discrete time series. Let $x = (x_0, \dots, x_N) \in \mathbb{R}^{d \times (N+1)}$ be a d -dimensional time series of length $N + 1$. Once specifying the Lie algebra \mathfrak{g} and $M \in L(\mathbb{R}^d, \mathfrak{g})$, one can define the development of x under M via the continuous lift of x by linear interpolation. Indeed, we parameterise the linear map $M \in L(\mathbb{R}^d, \mathfrak{g})$ of the development \mathcal{D}_M by its linear coefficients $\theta \in \mathfrak{g}^d$. More precisely, given $\theta = (\theta_1, \dots, \theta_d) \in \mathfrak{g}^d$, define $M_\theta : \mathbb{R}^d \ni x = (x^{(1)}, \dots, x^{(d)}) \mapsto \sum_{j=1}^d \theta_j x^{(j)} \in \mathfrak{g}$. We propose as follows the trainable path development layer, which is constructed in a recursive fashion.

Definition 3.1 (Path development layer). Fix a matrix group G with Lie algebra \mathfrak{g} . The path development layer is defined as a map $\mathcal{D}_\theta : \mathbb{R}^{d \times (N+1)} \rightarrow G^{N+1}$ [or G , resp.] : $x = (x_1, \dots, x_N) \mapsto z = (z_1, \dots, z_N)$ [or z_N , resp.] such that for each $n \in \{0, \dots, N-1\}$,

$$z_{n+1} = z_n \exp(M_\theta(x_{n+1} - x_n)), \quad z_0 = \mathrm{Id}_m. \quad (6)$$

Here \exp is the matrix exponential, G^{N+1} is the $(N + 1)$ -fold Cartesian product of G , and $\theta \in \mathfrak{g}^d$ are trainable model weights.

Remark 3.2. Eq. (6) arises from the multiplicative property of the development (Lemma 2.4) and the explicit solution of a linear path (Example 2.3). The output of development at step n , *i.e.*, z_n , admits an analytic formula $z_n = \prod_{i=1}^n \exp(M_\theta(x_i - x_{i-1}))$.

The recurrence structure of the development in Eq. (6) resembles that of the recurrent neural network (RNN) and the signature layer. In contrast to RNN, however, our path development layer does not require a fully connected neural network to construct the hidden neurons. Also, in comparison with the deterministic signature layer, it has trainable weights and is data-adaptive.

Remark 3.3. When choosing the matrix Lie algebra $\mathfrak{g} \subset \mathfrak{gl}(m, \mathbb{F})$, the resulting development feature is embedded in $GL(m, \mathbb{F})$. Note that $\dim_{\mathbb{F}} GL(m, \mathbb{F}) = m^2$, which is independent of the path dimension d . This is in stark contrast with the signature, whose range (at truncated order n) has dimension depending geometrically on d .

The development layer allows for both sequential output $z = (z_i)_{i=0}^N \in G^{N+1}$ and static output $z_N \in G$. Its forward evaluation is summarised in Algorithm 1.

Algorithm 1 Forward Pass of Path Development Layer

- 1: **Input:** $\theta \in \mathfrak{g}^d \subset \mathbb{R}^{m \times m \times d}$ (Model parameters),
 - 2: $x = (x_0, \dots, x_N) \in \mathbb{R}^{d \times (N+1)}$ (input time series),
 - 3: $m \in \mathbb{N}$ (order of the matrix Lie algebra).
 - 4: (d, N) are the feature and time dimensions of x , respectively.
 - 5: $z_0 \leftarrow \text{Id}_m$
 - 6: **for** $n \in \{1, \dots, N\}$ **do**
 - 7: $z_n \leftarrow z_{n-1} \exp(M_\theta(x_n - x_{n-1}))$
 - 8: **end for**
 - 9: **Output:** $z = (z_0, \dots, z_N) \in G^{N+1} \subset \mathbb{R}^{m \times m \times (N+1)}$ (sequential output) or $z_N \in G \subset \mathbb{R}^{m \times m}$ (static output).
-

3.2 Model parameter optimisation

Now we shall introduce a method for optimising model parameters of the development layer. Our proposed method not only effectively leverages the Lie group-valued output of the development through trivialisation, but also explores the recurrence structure of the development to enable efficient gradient computation via backpropagation through time.

More specifically, consider differentiable scalar field $\psi : G^{N+1} \rightarrow \mathbb{R}$ and an input $x := (x_n)_{n=0}^N \in \mathbb{R}^{N+1}$. We aim to find optimal parameters θ^* such as to minimise $\psi(\mathcal{D}_\theta(x))$; in formula,

$$\theta^* = \arg \min_{\theta \in \mathfrak{g}^d} \psi(\mathcal{D}_\theta(x)),$$

where \mathcal{D}_θ is the development layer defined in (6). Without loss of generality, we focus on the case where the output is the full sequence of path development. Unfortunately, gradient descent in Euclidean spaces is not directly applicable in our setting, due to the Lie group structure of the output.

To address this challenge, we adapt the method of trivialisation to facilitate gradient computations. First let us fix some notations. We denote $z := (z_n)_{n=0}^N \in G^{N+1}$ as the input variable of the differentiable scalar field $\psi : G^{N+1} \rightarrow \mathbb{R}$. Meanwhile, as before, z is also the output of the development layer \mathcal{D}_θ , whose input is $x = (x_n)_{n=0}^N \in \mathbb{R}^{d \times (N+1)}$. The variables z_n have the recursive structure $z_n = z_{n-1} \cdot \exp(M_{\theta_n}(\Delta x_n))$; see Eq. (6), wherein the independent variable at the n^{th} step is $\theta_n \in \mathfrak{g}^d$. We also introduce the projection:

$$\mathbf{pr}_i : G^{N+1} = G \times \dots \times G \longrightarrow G, \quad (g_0, \dots, g_N) \longmapsto g_i.$$

The notation \mathbf{pr}_i is chosen to distinguish from the projection π_k onto the k^{th} -level truncation of the signature (see Eq. (3)) and the projection from square matrices onto \mathfrak{g} (see Eq. (8)). Then for $\psi : G^{N+1} \rightarrow \mathbb{R}$, we identify $(\mathbf{pr}_i)_\# d\psi$ with a 1-form on G^{N+1} , by viewing the range TG of d as $\{0\} \oplus \dots \oplus \{0\} \oplus TG \oplus \{0\} \oplus \dots \oplus \{0\}$. Intuitively one may view $(\mathbf{pr}_i)_\# d\psi$, the pushforward of $d\psi$ via \mathbf{pr}_i , as the i^{th} partial derivative of ψ . Furthermore, we introduce the *Step- i update function*:

$$\mathfrak{S}_i : G \longrightarrow G, \quad \mathfrak{S}_i(z_{i-1}) := z_i \quad \text{for } i \in \{1, 2, \dots, N\}.$$

Also, define $\tilde{\psi}_n : G \rightarrow \mathbb{R}$ for $n \in \{0, 1, \dots, N-1\}$ via

$$\tilde{\psi}_n(z_n) := \psi\left(z_0, \dots, z_n, \mathfrak{S}_{n+1}(z_n), \mathfrak{S}_{n+2} \circ \mathfrak{S}_{n+1}(z_n), \dots, \mathfrak{S}_N \circ \dots \circ \mathfrak{S}_{n+1}(z_n)\right). \quad (7)$$

In other words, $\tilde{\psi}_n$ is simply ψ regarded as a function in the Step- n variable z_n , assuming that z_1, \dots, z_n have already been specified and choosing the subsequent variables z_{n+1}, \dots, z_N according to z_n .

We shall establish two lemmas that are key to our backpropagation algorithm of the development layer. First, the recurrence structure for z_n in (6) allows us to compute $d_{z_n} \tilde{\psi}_n$ effectively, also in a recursive manner:

Lemma 3.4 (Recurrence structure of gradient w.r.t z_n). *Let $x \in \mathbb{R}^{d \times (N+1)}$ and $z = (z_0, \dots, z_N) \in G^{N+1}$ be as before, where G is a matrix Lie group. Let $\psi : G^{N+1} \rightarrow \mathbb{R}$ be a smooth scalar field and $\tilde{\psi}_n$ be as in Eq. (7). Then, for each $n \in \{1, \dots, N\}$, we have*

$$d_{z_n} \tilde{\psi}_n = (\mathbf{pr}_n)_\# d\psi \Big|_{z_n} + d_{z_{n+1}} \tilde{\psi}_{n+1} \cdot \exp(M_{\theta_{n+1}}(\Delta x_{n+1})).$$

Here $\Delta x_{n+1} := x_{n+1} - x_n$ and \cdot is the matrix multiplication.

We need one further notation: for $z = (z_0, \dots, z_N) \in G^{N+1}$ as above, we write $\mathcal{Z} = (\mathcal{Z}_0, \dots, \mathcal{Z}_N)$ to denote $\mathcal{Z}_n(\theta_n) = z_n$ for $\theta_n \in \mathfrak{g}^d$. That is, one regards each z_n as a map $\mathfrak{g}^d \rightarrow G$. Then we set $\mathcal{Z}(\theta) := (\mathcal{Z}_0(\theta), \dots, \mathcal{Z}_N(\theta))$, namely that \mathcal{Z} equals $\mathcal{Z}_0 \oplus \dots \oplus \mathcal{Z}_N$ restricted to the multi-diagonal $\{(\theta, \dots, \theta) : \theta \in \mathfrak{g}^d\} \subset G^{N+1}$. In this way, Eq. (6) becomes

$$\mathcal{Z}_n(\theta_n) = z_{n-1} \cdot \exp\{M_{\theta_n}(\Delta x_n)\} \quad \text{for each } n \in \{1, 2, \dots, N\}.$$

With the notation above, we introduce a lemma that will allow us to compute the gradient of the Lie algebra-valued parameters in our development layer by adapting the method of trivialisation.

Lemma 3.5 (Gradient w.r.t θ). *Let $x \in \mathbb{R}^{d \times (N+1)}$, $z = (z_0, \dots, z_N) \in G^{N+1}$, $\psi : G \rightarrow \mathbb{R}$, $\theta_n \in \mathfrak{g}^d$, and $\mathcal{Z}_n : \mathfrak{g}^d \rightarrow G$ be as above. Denote by $d_{\text{HS}} := \text{tr}(A^\top B)$ as the metric associated to the Hilbert–Schmidt norm on the matrix Lie algebra \mathfrak{g} . For each $\theta \in \mathfrak{g}^d$, the gradient $\nabla_\theta(\psi \circ \mathcal{Z}) \in T_\theta \mathfrak{g}^d \cong \mathfrak{g}^d$ (with respect to a metric arising naturally from d_{HS}) satisfies the following:*

$$\nabla_\theta(\psi \circ \mathcal{Z}) = \sum_{n=1}^N \nabla_{\theta_n}(\tilde{\psi}_n \circ \mathcal{Z}_n) \Big|_{\theta_n=\theta},$$

where

$$\nabla_{\theta_n}(\tilde{\psi}_n \circ \mathcal{Z}_n) = d_{\mathfrak{m}_n(\theta_n)^\top} \exp(\nabla_{z_n} \tilde{\psi}_n \cdot z_{n-1}) \otimes \Delta x_n.$$

Here we denote $\mathfrak{m}_n(\theta_n) := M_{\theta_n}(\Delta x_n)$. Also, as before, $\Delta x_n := x_n - x_{n-1}$ and \cdot is the matrix multiplication.

We defer the proof of Lemma 3.4 and Lemma 3.5 to Appendix B. These two lemmas are crucial to our proposal of the backpropagation algorithm of the development layer. It mimics the backpropagation through time of the RNNs and involves the differential of the exponential map, which in turn can be computed efficiently through Lemma 2.13.

To formally describe the backpropagation algorithm, we introduce the projection map Proj and the embedding function $\hat{\Psi}$ as follows. Given a matrix algebra \mathfrak{g} , we view it as a subalgebra of $\mathfrak{gl}(m, \mathbb{C})$ for some m . Write

$$\text{Proj} : \mathfrak{gl}(m, \mathbb{C}) \longrightarrow \mathfrak{g} \tag{8}$$

for the nearest point projection, where $\mathfrak{gl}(m, \mathbb{C})$ is a Hilbert space equipped with the Hilbert–Schmidt norm. We embed the function $\Psi : G^{N+1} \rightarrow \mathbb{R}$ to the map $\hat{\Psi} : \mathfrak{gl}(m, \mathbb{C})^{N+1} \rightarrow \mathbb{R}$ such that $\hat{\psi}(y) = \psi(y)$, $\forall y = (y_0, \dots, y_N) \in G^{N+1} \subset \mathfrak{gl}(m, \mathbb{C})^{N+1}$. As $\mathfrak{gl}(m, \mathbb{C})^{N+1}$ is a vector space, we adopt the convention of the partial derivatives and total derivative of $\hat{\psi}$, i.e. $\partial_{y_i} \hat{\psi}$, $d_{y_i} \hat{\psi}$ denoting the partial derivative and total derivative of $\hat{\psi}$ w.r.t y_i , respectively, $\forall i \in \{0, 1, \dots, N\}$. The backpropagation algorithm of path development is as follows:

Algorithm 2 Backward Pass of Path Development Layer

- 1: **Input:** $x = (x_0, \dots, x_N) \in \mathbb{R}^{(N+1) \times d}$ (input time series), $z = (z_0, \dots, z_N) \in G^{N+1}$ (output series by the forward pass), $\theta = (\theta_1, \dots, \theta_d) \in \mathfrak{g}^d \subset \mathbb{R}^{m \times m \times d}$ (model parameters), $\eta \in \mathbb{R}$ (learning rate), $\hat{\psi} : \mathfrak{gl}(m, \mathbb{C})^{N+1} \rightarrow \mathbb{R}$ (loss function)
 - 2: Initialize $a \leftarrow 0$.
 - 3: Initialize $\mathfrak{m} \leftarrow 0$. $\triangleright \mathfrak{m}$ represents $M_\theta(\Delta x_n)$
 - 4: Initialize $\omega \leftarrow 0$. $\triangleright \omega$ represents $\nabla_\theta(\psi \circ \mathcal{Z})$
 - 5: **for** $n \in \{N, \dots, 1\}$ **do**
 - 6: Compute $a \leftarrow \partial_{y_n} \hat{\psi}|_{y=z} + a \cdot \mathfrak{m}$
 - 7: Compute $\mathfrak{m} \leftarrow M_\theta(\Delta x_n)$.
 - 8: Compute $\omega \leftarrow \omega + d_{\mathfrak{m}^\top} \exp(a \cdot z_{n-1}) \otimes \Delta x_n$ \triangleright by Lemma 3.5 and Lemma 2.13.
 - 9: **end for**
 - 10: $\theta \leftarrow \theta - \eta \cdot \omega$.
 - 11: **for** $i \in \{1, \dots, d\}$ **do**
 - 12: $\theta_i \leftarrow \text{Proj}(\theta_i) \in \mathfrak{g}$.
 - 13: **end for**
 - 14: **Output:** return θ (updated model parameter)
-

Our implementation, built on top of the fast machine-precision approximation to the matrix exponential and its differential (Al-Mohy and Higham [2009, 2010]), allows us to evaluate and train the development layer efficiently. Also

the implementation of the development layer can be flexibly adapted to general matrix Lie algebra. The full list of matrix Lie algebras associated with the implemented development layers can be found in Appendix B. The code of the development layer and numerical examples for the reproducibility of the results in the next section are available at <https://github.com/PDevNet/DevNet>.

4 Numerical Experiments

In this section, we validate the performance of the proposed development layer (DEV) and the hybrid model constructed by the LSTM and the development layer (LSTM+DEV) by benchmarking against a variety of models, including the signature model and the long short-term memory (LSTM), as baselines as well as state-of-the-art (STOA) models of each tasks. DEV(SO), DEV(Sp), and DEV(SE) represent developments with special orthogonal, real symplectic, and special Euclidean matrix Lie groups, respectively. The loss function is chosen, in the standard way, to be the cross entropy for the first two classification tasks and the mean squared error (MSE) for the last regression task. For fair comparison, every model has a comparable number of parameters. The full implementation details of numerical experiments, including train/validation/test split, models, hyperparameters, and optimizer, can be found in Appendix C.

4.1 Speech Command dataset

We first demonstrate the performance of the path development network on the Speech Commands dataset (Warden [2018]) as an example of high-dimensional long time series. We follow Kidger et al. [2020] to precompute mel-frequency cepstrum coefficients of the audio recording and consider a balanced classification task of predicting a spoken word. This processed dataset consists of 34975 samples of secondly audio recordings, represented in a regularly spaced time series of length 169 and path dimension 20.

Dimension reduction of the path development. To make comparison between the signature and development features, we apply linear model to both features on the Speech Command dataset and compare the corresponding classification accuracy and feature dimension. In Section 4.1, the curve of test accuracy against feature dimension of the development (Red) is consistently above that of the signature (Blue). To achieve comparable test accuracy, the required dimension of the development is much less than that of the signature, thanks to the data-adaptive nature of the development layer. The development layer with matrix Lie group of order 30 achieves an accuracy about 86% of that of the signature, but with dimension reduced by a factor of 9 (900 v.s. 8420).

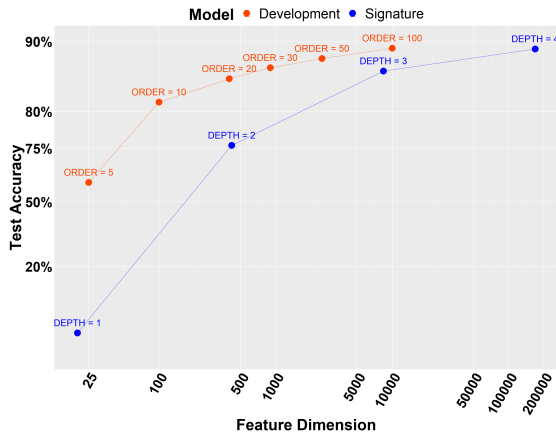


Figure 3: Test accuracy v.s. the feature dimension curves of the linear models using the development and signature representation on Speech Commands dataset. See full results in Table 4.

State-of-the-art performance. We first compare the proposed development model with other continuous time series model baselines, including GRU-ODE (De Brouwer et al. [2019]), ODE-RNN (Rubanova et al. [2019]), and NCDE (Kidger et al. [2020]). Our model significantly outperforms GRU-ODE and ODE-RNN on this task, whilst achieve comparable test accuracy with NCDE. The average accuracy of NCDE is 1.9% higher than our development model. However, the standard deviation of the NCDE model is 2.5%, higher than that of the development model (0.1%), thus making the accuracy difference of these two models insignificant. Note that NCDEs fully parameterize the vector field

of the controlled differential equations (CDEs) by a neural network, while our proposed development satisfies *linear* CDEs with trainable weights constrained in the matrix Lie algebra. The difference in complexities of the relevant CDEs may contribute to the higher average test accuracy and higher variation of the prediction by NCDE.

MODEL	TEST ACCURACY	# PARAMS
GRU-ODE	47.9% \pm 2.9%	89K
ODE-RNN	65.9% \pm 35.6%	89K
NCDE	89.8% \pm 2.5%	89K
FLEXTCN	97.7 %	373K
LSTM	95.7% \pm 0.2%	88K
SIGNATURE	85.7% \pm 0.1%	84K
DEV(SO)	87.9% \pm 0.1%	87K
LSTM+DEV(SO)	96.8% \pm 0.1%	86K

Table 1: Test accuracies (mean \pm std, computed across 5 runs) on the Speech Commands dataset

Compared with the strong baseline LSTM, the development layer alone has a lower accuracy by 7.8%. However, our hybrid model (LSTM+DEV) further improves the LSTM performance by 0.9%. The LSTM+DEV model achieves 96.8% test accuracy, which is slightly lower than that of the state-of-the-art FLEXTCN (Romero et al. [2021]). However, involving only a quarter of parameters of the latter, our model is significantly more compact than FLEXTCN.

4.2 Character Trajectories dataset

Next we investigate the performance of the development network on irregular time series. We consider the Character Trajectories from the UEA time series classification archive (Bagnall et al. [2018]). This dataset consists of Latin alphabet characters written in a single stroke with their 2-dimensional positions and pen tip force. There are 2858 time series with a constant length of 182 and 20 unique characters to classify. Following the approach in Kidger et al. [2020], we randomly drop 30%, 50%, or 70% of the data in the same way for every model and every repeat, which results in irregular sampled time series.

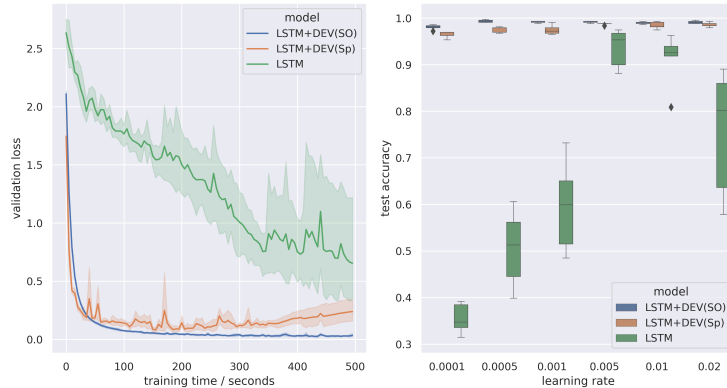
State-of-the-art accuracy. Similar to Speech Commands dataset, the development layer itself outperforms the signature layer, whilst it still underperforms NCDE and LSTM in terms of test accuracy. However, the proposed hybrid model (LSTM+DEV) with special orthogonal group achieves the state-of-the-art accuracy, with around 0.6-0.7% and 0-1.1% performance gain in comparison to the best NCDE and CKCNN models, respectively.

Robustness to dropping data. Table 2 demonstrates that, as observed for other continuous time series models, the accuracy of DEV and LSTM+DEV remains similar across different drop rates, thus exhibiting robustness against data dropping and irregular sampling of time series. LSTM achieves competitive accuracy around 94% when dropping rate is relatively low, with a drastic performance decrease (6%) for the high drop rate (70%). However, adding the development layer, especially the one with special orthogonal group, significantly improves the robustness of LSTM to high drop rate.

Table 2: Test accuracies (mean \pm std, computed across 5 runs) on the Character Trajectories dataset.

MODEL	TEST ACCURACY		
	30%	50%	70%
GRU-ODE	92.6% \pm 1.6%	86.7% \pm 3.9%	89.9% \pm 3.7%
ODE-RNN	95.4% \pm 0.6%	96.0% \pm 0.3%	95.3% \pm 0.6%
NCDE	98.7% \pm 0.8%	98.8% \pm 0.2%	98.6% \pm 0.4%
CKCNN	99.3%	98.8%	98.1%
LSTM	94.0% \pm 3.9%	94.6% \pm 2.0%	87.8% \pm 6.3%
SIGNATURE	92.1% \pm 0.2%	92.3% \pm 0.5%	90.2% \pm 0.4%
DEV (SO)	92.7% \pm 0.6%	92.6% \pm 0.9%	91.9% \pm 0.9 %
LSTM+DEV (SO)	99.3% \pm 0.3%	99.3% \pm 0.1%	99.2% \pm 0.3%
LSTM+DEV (SP)	97.7% \pm 0.2%	97.7% \pm 0.2%	97.4% \pm 0.4%

Figure 4: The comparison plot of LSTM and LSTM+DEV on Character Trajectories with 30% drop rate. (Left) The evolution of validation loss against training time. The mean curve with \pm std indicated by the shaded area is computed over 5 runs. (Right) The boxplot of the validation accuracy for varying learning rate.



Improvement of training LSTMs by Development Layer (LSTM+DEV). Apart from model robustness, the additional development layer improves the LSTM in terms of (1), training stability and convergence; and (2), less need for hyper-parameter tuning. This has led to better model performance with faster training.

Training Stability and convergence. Figure 4 (Left) and Figure 6 in Appendix show the oscillatory evolution of the loss and accuracy of the LSTM model during training, which can be significantly stabilised by adding development layers DEV(SO) and DEV(Sp). In particular, the performance of DEV(SO) is better than that of DEV(Sp) in terms of both training stability and prediction accuracy. It suggests that the development layer may help with saturation of hidden states of the LSTMs and resolving of the gradient vanishing/exploding issues, because of the boundedness of intermediate gradients resulted from the Lie group-valued output of the development. Hence, it can serve as an effective means for alleviating long temporal dependency issues of the LSTM. Moreover, our hybrid model has a much faster training convergence rate than LSTM.

Sensitivity of learning rate. Figure 4 (Right) shows that the LSTM performance is highly sensitive to the learning rate. So, extensive, time-consuming hyper-parameter tuning is a must to ensure high performance of the LSTM model. However, the LSTM+DEV model training is much more robust to the learning rate, leading to less hyper-parameter tuning and consistently superior performance over the LSTM.

Training time. The LSTM+DEV(SO) with SOTA performance reported in Table 2 takes 20% less time per epoch than the baseline LSTM for model training. Both models have comparable number of parameters. See Appendix C.3 for details on model architectures.

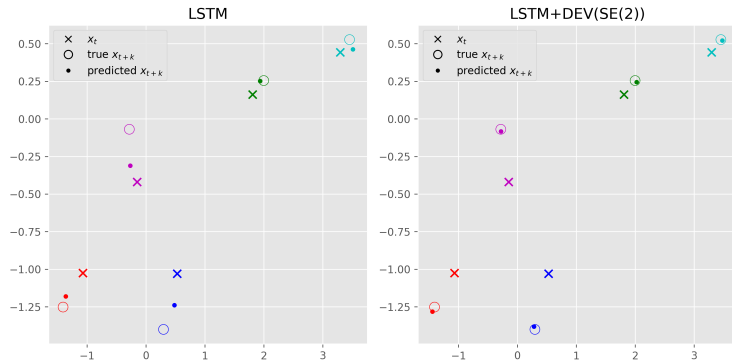
4.3 N -body simulations

Finally, we demonstrate the efficacy of the development network by utilizing its group structure to predict 2-D interacting particle systems. Following Kipf et al. [2018], we use the simulated dataset of 5 charged particles and consider a regression task of predicting the future k -step location of the particles. The input sequence consists of the location and velocity of particles in the past 500 steps. As coordinate transforms from the current location x_t to the future location x_{t+k} lie in $SE(2)$ (the special Euclidean group), we propose to use the LSTM+DEV with $SE(2)$ -representation to model such transforms. Details of data simulation and model architecture can be found in Appendix C.4. To benchmark our proposed method, we consider two other baselines: (1) the current location (static) and (2) the LSTM model. To demonstrate the usefulness of the Lie algebra choice, we compare our method with LSTM+DEV(SO(2)).

As shown in Table 3, the proposed LSTM+DEV(SE(2)) consistently and significantly outperforms both baselines and LSTM+DEV(SO(2)) in terms of MSE for varying $k \in \{100, 300, 500\}$. Figure 5 provides a visual demonstration to show the superior performance of the estimator of future location by our LSTM+DEV(SE(2)) in comparison to the strongest baseline LSTM, thus manifesting the efficacy of incorporating development layers with inherited group structures in learning tasks.

Table 3: Test MSE (mean \pm std, computed across 5 runs) on the N -body simulation dataset

PREDICTION STEPS	TEST MSE (1e-3)		
	100	300	500
STATIC	7.79	61.1	157
LSTM	3.54 ± 0.22	22.1 ± 1.5	63.2 ± 1.4
LSTM+DEV(SO(2))	5.50 ± 0.01	47.5 ± 0.19	128 ± 0.58
LSTM+DEV(SE(2))	0.505 ± 0.01	6.94 ± 0.16	25.6 ± 1.5

Figure 5: Prediction comparison between LSTM (left) and LSTM+DEV (SE(2)) (right) in the 5-body simulation problem. Plots show current location x_t (also static estimator), ground truth future location (x_{t+300}), and predicted locations from both models.

5 Conclusion and Future work

In this paper, we propose a novel, trainable path development layer with finite-dimensional matrix Lie group for sequential data tasks. Empirical experiments demonstrate that the development layer, thanks to its algebraic/geometric structure and recurrent nature, can help improve the performance of the LSTM models, leading to the state-of-the-art hybrid model with fast training.

Like RNN-type models, despite its fast training and evaluation, the computation of the development layer may suffer from the memory bottleneck, which may be alleviated by memory optimisation schemes designed for RNN-type models. See Zheng et al. [2020].

Although the exposition of our work focuses on matrix Lie groups, our methodology and implementation of the development layer can be naturally extended to general Lie groups and their group representations. Following recent work of incorporating Lie group representations with neural networks (Fuchs et al. [2020], Thomas et al. [2018]), it opens doors to utilise representations to increase expressiveness of the development layer and further enhance its performance.

Finally, the Lie group structure and the linear controlled differential equations satisfied by the development may offer potential opportunities for the explainability of our model, which merits further investigations in the future.

Acknowledgement

HN is supported by the EPSRC under the program grant EP/S026347/1 and the Alan Turing Institute under the EPSRC grant EP/N510129/1. LH is supported by University College London and the China Scholarship Council under the UCL-CSC scholarship (No. 201908060002).

The authors extend their gratitude to Terry Lyons for insightful discussion. HN would like to thank Kevin Schlegel and Jijie Tao for proofreading the paper. HN is also grateful to Jing Liu for her help with Figure 1.

A The development of a path

A.1 Connection with signature

Recall that $\mathcal{V}_1([0, T], \mathbb{R}^d)$ denote the space of continuous paths $[0, T] \rightarrow \mathbb{R}^d$ of bounded 1-variation and \mathfrak{g} is a Lie algebra.

Lemma A.1 (Lemma 2.6). *Let $X \in \mathcal{V}_1([0, T], \mathbb{R}^d)$ and $M \in L(\mathbb{R}^d, \mathfrak{g})$. Then $D_M(X) = \widetilde{M}(S(X))$.*

Proof. By definition of the development of the path X , $D_M(X)$ is the endpoint of $(Z_t)_{t \in [0, T]}$, which satisfies the linear controlled differential equation

$$dZ_t = Z_t M(dX_t), \quad Z_0 = \text{Id}.$$

By Picard iteration, one obtains

$$D_M(X) := Z_T = \text{Id} + \sum_{n \geq 1} \int_{0 < t_1 < \dots < t_n < T} M(dX_{t_1}) \cdots M(dX_{t_n}).$$

Thus, by linearity of M , the right-hand side of the above equation coincides with $\widetilde{M}(S(X))$. \square

A.2 Dimension comparison with signature

The dimension of the signature of a d -dimensional path of depth k is $\frac{d^{k+1}-1}{d-1}$ if $d \geq 2$ and k if $d = 1$. When specifying the Lie algebra \mathfrak{g} of the development as a matrix algebra, the dimension of development of order m is m^2 (independent of d). The dimension of trainable weights of the development layer with static output is dm^2 , while the signature layer does not have any trainable parameter.

A.3 Invariance under time-reparameterisation

Lemma A.2 (Lemma 2.7). *Let $X \in \mathcal{V}_1([0, T], \mathbb{R}^d)$ and let λ be a non-decreasing function from $[0, S]$ onto $[0, T]$. Define $X_t^\lambda := X_{\lambda_t}$ for $t \in [0, T]$. Then for all $M \in L(\mathbb{R}^d, \mathfrak{g})$*

$$D_M(X_{\lambda_s, \lambda_t}) = D_M(X_{s, t}^\lambda).$$

Proof. It follows directly from Lemma 2.6 and the invariance under time reparameterisation of the signature. See Chevyrev and Kormilitzin [2016]. \square

A.4 Universality

Definition A.3 (Lie algebra Representation). Let \mathfrak{g} be a Lie algebra and W be a vector space. Denote by $\mathfrak{gl}(W)$ the space of the endomorphisms of W equipped with the bracket $[\sigma_1, \sigma_2] := \sigma_1 \circ \sigma_2 - \sigma_2 \circ \sigma_1$. A representation of \mathfrak{g} on V , denoted by ρ , is a Lie algebra homomorphism $\mathfrak{g} \rightarrow \mathfrak{gl}(V)$; that is, a linear map with

$$\rho([X_1, X_2]) = [\rho(X_1), \rho(X_2)] \quad \text{for all } X_1, X_2 \in \mathfrak{g}.$$

The following universality property is essentially established in §4, Chevyrev and Lyons [2016].

Theorem A.4 (Universality of path development). *Let \mathcal{G} be the space of group-like elements in the tensor algebra $T((\mathbb{R}^d))$. For any compact subset $\mathcal{K} \subset \mathcal{G}$, every continuous function from \mathcal{K} to \mathbb{C} can be uniformly approximated by a sequence of maps $(L_j \circ \widetilde{M}_j)_{j=1}^\infty$, where $\widetilde{M}_j \in L(\mathcal{G}, \mathfrak{gl}(m, \mathbb{C}))$ is the algebra homomorphism corresponding naturally to $M_j \in L(\mathbb{R}^d; \mathfrak{gl}(m, \mathbb{C}))$ for some $m \geq 1$, and $L_j : \mathfrak{gl}(m, \mathbb{C}) \rightarrow \mathbb{C}$ is a linear map.*

Proof. Consider

$$\mathcal{A} := \text{Hom} \left(T((\mathbb{R}^d)); \bigoplus_{m=1}^\infty \mathfrak{gl}(m, \mathbb{C}) \right)$$

and restrictions to the domain of group-like elements — $\mathcal{A}_{\mathcal{L}\mathcal{G}} := \{\rho_{\mathcal{L}\mathcal{G}} : \rho \in \mathcal{A}\}$. Here Hom denotes Banach algebra homomorphism over \mathbb{C} , with tensor algebra endowed with the natural topology associated with the projective tensor

norm (see Definition 2.1 in Chevyrev and Lyons [2016]) and $\mathfrak{gl}(m, \mathbb{C})$ with the Hilbert–Schmidt norm. Moreover, on \mathcal{A} the unit is the trivial representation; the product is given by $\rho_1 \otimes \rho_2(x) := \rho_1(x) \otimes \rho_2(x)$ for $\rho_1, \rho_2 \in \mathcal{A}$; the addition is just defined componentwise; and the involution in \mathcal{A} corresponds to the dual representation, namely that $\rho^*(x) := -[\rho(x)]^*$ (the adjoint matrix) for $\rho \in \mathcal{A}$.

As a side remark, it may appear odd that the product in \mathcal{A} has the structure of tensor product of *group* representations instead of *Lie algebra* representations. This is intentionally designed to make $\mathcal{A} \llcorner_{\mathcal{G}}$ a *Hopf algebra* representation of the space of group-like elements \mathcal{G} . Indeed, one characterisation of \mathcal{G} is that

$$\mathcal{G} = \{x \in T((\mathbb{R}^d)) \setminus \{0\} : \blacktriangle(x) = x \otimes x\},$$

where \blacktriangle is the Hopf algebra coproduct on the tensor algebra, extended from $\blacktriangle(v) = v \otimes \mathbf{1} + \mathbf{1} \otimes v$ on \mathbb{R}^d . Then we have $(\rho_1 \otimes \rho_2)(x) \equiv (\rho_1 \otimes \rho_2)[\blacktriangle(x)]$ in this provision. Also, the minus sign in the dual representation corresponds to the antipode of the Hopf algebra.

Next, consider the subset

$$\mathcal{A}_1 := \left\{ \varrho \in \mathcal{A} \llcorner_{\mathcal{G}} \text{ that arises from } L \left(\mathbb{R}^d, \bigoplus_{m=1}^{\infty} \mathfrak{gl}(m, \mathbb{C}) \right) \right\}.$$

In other words, \mathcal{A}_1 consists of those \widetilde{M} extended by naturality from some $M \in L(\mathbb{R}^d, \mathfrak{gl}(m, \mathbb{C}))$, in the same notation as before. By definitions of \widetilde{M} and of tensor product representations in $\mathcal{A} \llcorner_{\mathcal{G}}$, one may straightforwardly verify for $x \in \mathcal{G}$ that

$$\left(\widetilde{M}_1 \otimes \widetilde{M}_2 \right) (x) = \widetilde{M_1 \otimes M_2}(x).$$

In addition, the closure of \mathcal{A}_1 under involution is clear. Thus \mathcal{A}_1 is a subrepresentation (of Hopf algebras). Moreover, in view of Theorem 2.9, \mathcal{A}_1 separates points over \mathcal{G} .

Now we are ready to conclude the proof. As \mathcal{G} is Hausdorff (see Corollary 2.4 in Chevyrev and Lyons [2016]) and \mathcal{A}_1 contains the constant 1 by considering representations evaluated at $\mathbf{1} = (1, 0, 0, \dots) \in \mathcal{G}$, we can invoke the Stone–Weierstrass theorem — namely that for a compact Hausdorff space X , if $S \subset C^0(X, \mathbb{C})$ separates points, then the complex unital $*$ -algebra generated by S is dense in $C^0(X, \mathbb{C})$ — to conclude that the linear functionals $(\mathcal{A}_1 \llcorner_{\mathcal{K}})'$ is dense in $C^0(\mathcal{K}; \mathbb{C})$ for any compact $\mathcal{K} \subset \mathcal{G}$. \square

Remark A.5. In the statement Theorem A.4 we may replace $\mathfrak{gl}(m, \mathbb{C})$ by any subalgebra \mathfrak{k} of the unitary Lie algebra $\mathfrak{u}(m, \mathbb{C})$. The proof is essentially the same, as the Hopf algebra representations of \mathcal{G} into $\bigoplus_{\dim \mathfrak{k}=1}^{\infty} \mathfrak{k}$ remains a complex unital $*$ -algebra separating points over \mathcal{G} .

B Backpropagation of the development layer

Let us first prove Lemma 3.4, reproduced below:

Lemma B.1 (Recurrence structure of gradient w.r.t z_n). *Let $x \in \mathbb{R}^{d \times (N+1)}$ and $z = (z_0, \dots, z_N) \in G^{N+1}$ be as before, where G is a matrix Lie group. Let $\psi : G^{N+1} \rightarrow \mathbb{R}$ be a smooth scalar field and $\widetilde{\psi}_n$ be as in Eq. (7). Then, for each $n \in \{1, \dots, N\}$, we have*

$$d_{z_n} \widetilde{\psi}_n = (\mathbf{pr}_n)_{\#} d\psi \Big|_{z_n} + d_{z_{n+1}} \widetilde{\psi}_{n+1} \cdot \exp(M_{\theta_{n+1}}(\Delta x_{n+1})).$$

Here $\Delta x_{n+1} := x_{n+1} - x_n$ and \cdot is the matrix multiplication.

Proof. We first consider a more general statement: let \mathcal{M} and \mathcal{N} be differentiable manifolds, let $f : \mathcal{M} \rightarrow \mathcal{N}$ be a smooth function, and let $\widetilde{\psi} : \mathcal{M} \rightarrow \mathbb{R}$ be a scalar field factors through the graph of f . That is, there is a smooth function $\psi : \mathcal{M} \times \mathcal{N} \rightarrow \mathbb{R}$ such that $\widetilde{\psi}(x) = \psi(x, f(x))$ for each $x \in \mathcal{M}$. Then we have the following identity on $T^*\mathcal{M}$:

$$d\widetilde{\psi} = (\mathbf{pr}_I)_{\#} d\psi + \left[(\mathbf{pr}_{II})_{\#} d\psi \right] \circ df. \quad (9)$$

Here we view $(\mathbf{pr}_I)_{\#} d\psi \in T^*\mathcal{M} \oplus \{0\}$ and $\left[(\mathbf{pr}_{II})_{\#} d\psi \right] \circ df \in \{0\} \oplus T^*\mathcal{M}$; the symbols \mathbf{pr}_I and \mathbf{pr}_{II} denote the canonical projections from $\mathcal{M} \times \mathcal{N}$ onto \mathcal{M} and \mathcal{N} , respectively.

The proof for Eq. (9) is straightforward. For functions $f_1 : E \rightarrow S_1$ and $f_2 : E \rightarrow S_2$ where E, S_1, S_2 are arbitrary sets, we denote $f_1 \oplus f_2 : E \rightarrow (S_1 \times S_2)$ as the function $(f_1 \oplus f_2)(x) := (f_1(x), f_2(x))$. In this notation one has

$$\tilde{\psi} = \psi \circ (\text{Id}_{\mathcal{M}} \oplus f).$$

Using the chain rule we then deduce that

$$d\tilde{\psi} = d\psi|_{\text{range}(\text{Id}_{\mathcal{M}} \oplus f)} \circ d(\text{Id}_{\mathcal{M}} \oplus f) = d\psi|_{\text{graph } f} \circ (\text{Id}_{T\mathcal{M}} \oplus df),$$

with $\text{Id}_{T\mathcal{M}} : T\mathcal{M} \rightarrow [T\mathcal{M} \cong T\mathcal{M} \oplus \{0\}]$ and $df : T\mathcal{M} \rightarrow [T\mathcal{N} \cong \{0\} \oplus T\mathcal{N}]$. This is tantamount to the right-hand side of Eq. (9) by the definition of \mathbf{pr}_I and \mathbf{pr}_{II} .

Let us now prove the lemma from the identity (9). Indeed, by taking \mathbf{pr}_n in place of \mathbf{pr}_I and $f = \mathfrak{S}_{n+1} \oplus (\mathfrak{S}_{n+2} \circ \mathfrak{S}_{n+1}) \oplus \dots \oplus (\mathfrak{S}_N \circ \dots \circ \mathfrak{S}_{n+2} \circ \mathfrak{S}_{n+1})$, where $\mathcal{M} = G$ and $\mathcal{N} = G^{N-n}$, we deduce that

$$\begin{aligned} d\tilde{\psi}_n &= (\mathbf{pr}_n)_\# d\psi + \left\{ (\mathbf{pr}_{n+1})_\# d\psi \right\} \cdot d\mathfrak{S}_{n+1} + \left\{ (\mathbf{pr}_{n+2})_\# d\psi \right\} \cdot d(\mathfrak{S}_{n+2} \circ \mathfrak{S}_{n+1}) \\ &\quad + \left\{ (\mathbf{pr}_N)_\# d\psi \right\} \cdot d(\mathfrak{S}_N \circ \dots \circ \mathfrak{S}_{n+2} \circ \mathfrak{S}_{n+1}) \\ &= (\mathbf{pr}_n)_\# d\psi + \left\{ (\mathbf{pr}_{n+1})_\# d\psi \right\} \cdot d\mathfrak{S}_{n+1} + \left\{ (\mathbf{pr}_{n+2})_\# d\psi \right\} \cdot d\mathfrak{S}_{n+2} \cdot d\mathfrak{S}_{n+1} \\ &\quad + \left\{ (\mathbf{pr}_N)_\# d\psi \right\} \cdot d(\mathfrak{S}_N \circ \mathfrak{S}_{N-1} \circ \dots \circ \mathfrak{S}_{n+2}) \cdot d\mathfrak{S}_{n+1}. \end{aligned}$$

Here we have used the fact that for $\mathcal{L}_g : G \rightarrow G$, $\mathcal{L}_g(h) := gh$, its differential $d\mathcal{L}_g$ is also the left-multiplication by g , which is given by matrix multiplication when \mathfrak{g} is a matrix algebra. The second equality follows from the chain rule.

On the other hand, that the terms in the right-most expression above possess a recursive structure too: by taking \mathbf{pr}_{n+1} in place of \mathbf{pr}_I and $f = \mathfrak{S}_{n+2} \oplus (\mathfrak{S}_{n+3} \circ \mathfrak{S}_{n+2}) \oplus \dots \oplus (\mathfrak{S}_N \circ \dots \circ \mathfrak{S}_{n+2})$ in Eq. (9), we have

$$(\mathbf{pr}_{n+1})_\# d\psi + \left\{ (\mathbf{pr}_{n+2})_\# d\psi \right\} \cdot d\mathfrak{S}_{n+2} + \left\{ (\mathbf{pr}_N)_\# d\psi \right\} \cdot d(\mathfrak{S}_N \circ \mathfrak{S}_{N-1} \circ \dots \circ \mathfrak{S}_{n+2}) = d\tilde{\psi}_{n+1}.$$

The above computations established the following equality on T^*G :

$$d\tilde{\psi}_n = (\mathbf{pr}_n)_\# d\psi + d\tilde{\psi}_{n+1} \cdot d\mathfrak{S}_{n+1}.$$

Thus, evaluating this identity at $z_n \in G$, we infer from the definition of the update function $\mathfrak{S}_{n+1}(z_n) = z_{n+1}$ that

$$d_{z_n} \tilde{\psi}_n = (\mathbf{pr}_n)_\# d\psi|_{z_n} + d_{z_{n+1}} \tilde{\psi}_{n+1} \cdot d_{z_n} \mathfrak{S}_{n+1}.$$

We can now complete the proof from the recurrence relation $z_{n+1} = z_n \cdot \exp(M_{\theta_{n+1}}(\Delta x_{n+1}))$ given in Eq. (6). \square

Recall the following from Lezcano-Casado [2019], Lezcano-Casado and Martinez-Rubio [2019]: consider a parameterisation map $\Phi : \mathcal{N} \rightarrow \mathcal{M}$ between Riemannian manifolds (\mathcal{M}, g_1) and (\mathcal{N}, g_2) . Denote the differential by $d\Phi : T\mathcal{N} \rightarrow T\mathcal{M}$ and the adjoint with respect to both metrics g_1, g_2 of $d\Phi$ by $d\Phi^* : T\mathcal{M} \rightarrow T\mathcal{N}$. Then the following can be shown immediately from the definition of gradient. See Lezcano-Casado [2019] for a proof.

Corollary B.2. *Let $\Phi : \mathcal{N} \rightarrow \mathcal{M}$ be a smooth map between Riemannian manifolds and $f : \mathcal{M} \rightarrow \mathbb{R}$. We have*

$$\nabla(f \circ \Phi) = d\Phi^*(\nabla f).$$

We now move on to a proof for Lemma 3.5, reproduced below:

Lemma B.3 (Gradient w.r.t θ). *Let $x \in \mathbb{R}^{d \times (N+1)}$, $z = (z_0, \dots, z_N) \in G^{N+1}$, $\psi : G \rightarrow \mathbb{R}$, $\theta_n \in \mathfrak{g}^d$, and $Z_n : \mathfrak{g}^d \rightarrow G$ be as above. Denote by $d_{\text{HS}} := \text{tr}(A^\top B)$ the metric associated to the Hilbert–Schmidt norm on the matrix Lie algebra \mathfrak{g} . For each $\theta \in \mathfrak{g}^d$, the gradient $\nabla_\theta(\psi \circ Z) \in T_\theta \mathfrak{g}^d \cong \mathfrak{g}^d$ (with respect to a natural metric arising from the d_{HS}) satisfies the following:*

$$\nabla_\theta(\psi \circ Z) = \sum_{n=1}^N \nabla_{\theta_n}(\tilde{\psi}_n \circ Z_n) \Big|_{\theta_n = \theta},$$

where

$$\nabla_{\theta_n}(\psi_n \circ Z_n) = d_{\mathfrak{m}_n(\theta_n)^\top} \exp(\nabla_{z_n} \tilde{\psi}_n \cdot z_{n-1}) \otimes \Delta x_n.$$

Here we denote $\mathfrak{m}_n(\theta_n) := M_{\theta_n}(\Delta x_n)$. Also, as before, $\Delta x_n := x_n - x_{n-1}$ and \cdot is the matrix multiplication.

Proof. The first statement follows directly from the definition of $\tilde{\psi}_n$ in Eq. (7).

To prove the second statement, we first compute the differential

$$\Xi := d_{\theta_n}(\tilde{\psi}_n \circ \mathcal{Z}_n)$$

for $\theta_n \in \mathfrak{g}^d$. Since $\Xi : T_{\theta_n} \mathfrak{g}^d \rightarrow \mathbb{R}$, we need to find for each vector field ξ over \mathfrak{g}^d the value $\Xi(\xi)$. Let us denote by $\mathcal{L}_{g_1} : G \rightarrow G$ for each $g_1 \in G$ the left regular action, *i.e.*, $\mathcal{L}_{g_1}(g_2) := g_1 g_2$. Then $z_n = \mathcal{L}_{z_{n-1}}(\exp(M_{\theta_n}(\Delta x_n)))$ describes the recurrence structure in Eq. (6); hence, we obtain

$$\Xi(\xi) := d_{\theta_n}(\tilde{\psi}_n \circ \mathcal{Z}_n)(\xi) = d_{\theta_n}((\tilde{\psi}_n \circ \mathcal{L}_{z_{n-1}}) \circ \exp(M_{\theta_n}(\Delta x_n)))(\xi)$$

To simplify the equation above, let us label $M_{\theta_n}(\Delta x_n) =: \mathfrak{m}_n(\theta_n)$ for $\mathfrak{m}_n : \mathfrak{g}^d \rightarrow \mathfrak{g}$. Then, applying the chain rule, one obtains

$$\begin{aligned} d_{\theta_n}((\tilde{\psi}_n \circ \mathcal{L}_{z_{n-1}}) \circ \exp(M_{\theta_n}(\Delta x_n)))(\xi) &= d_{\mathfrak{m}_n(\theta_n)}((\tilde{\psi}_n \circ \mathcal{L}_{z_{n-1}}) \circ \exp) \circ d_{\theta_n} \mathfrak{m}_n(\xi) \\ &= d_{\mathfrak{m}_n(\theta_n)}((\tilde{\psi}_n \circ \mathcal{L}_{z_{n-1}}) \circ \exp) \circ \mathfrak{m}_n(\xi). \end{aligned} \quad (10)$$

The second identity holds since \mathfrak{m} is a linear mapping; here we identify $T_{\theta} \mathfrak{g}^d \cong \mathfrak{g}^d$ and $T_{\mathfrak{m}(\theta)} \mathfrak{g} \cong \mathfrak{g}$, where $\mathfrak{m}_n(\theta) := \sum_{j=1}^d (\Delta x_n)^j \theta^j$ for $\theta = \sum_{j=1}^d \theta^j \mathbf{e}_j$, with $\{\mathbf{e}_j\}_{j=1}^d$ being the canonical basis for \mathbb{R}^d .

Now we proceed with the computation for the gradient $\nabla_{\theta_n} \tilde{\psi}_n \circ \mathcal{Z}_n$, which by definition is dual to the differential via canonical isomorphisms between tangent and cotangent bundles, *i.e.*, the ‘‘musical isomorphisms’’. To be precise, denote by $\alpha : T\mathfrak{g} \rightarrow T^*\mathfrak{g}$ and $\beta : T\mathfrak{g}^d \rightarrow T^*\mathfrak{g}^d$ such canonical isomorphisms. Since we are working with matrix Lie algebra \mathfrak{g} , we shall take α with respect to the metric d_{HS} associated to the Hilbert–Schmidt norm on \mathfrak{g} , and take β with respect to the metric \hat{d} associated to the ℓ^1 -norm nested with d_{HS} . Recall here that $d_{\text{HS}}(A, B) := \text{tr}(A^\top B)$ and $\hat{d}[(A_j)_1^d, (B_j)_1^d] := \sum_{j=1}^d d_{\text{HS}}(A_j, B_j)$. Then we infer from Eq. (10) that

$$\begin{aligned} \nabla_{\theta_n} (\tilde{\psi}_n \circ \mathcal{Z}_n) &= \beta^{-1}(d_{\theta_n}(\tilde{\psi}_n \circ \mathcal{Z}_n)) \\ &= \beta^{-1}(d_{\mathfrak{m}_n(\theta_n)}((\tilde{\psi}_n \circ \mathcal{L}_{z_{n-1}}) \circ \exp) \circ \mathfrak{m}_n) \end{aligned}$$

Denote by $\mathfrak{m}_n^* : T\mathfrak{g} \rightarrow T\mathfrak{g}^d$ the adjoint of \mathfrak{m}_n with respect to α and β above. It follows from Corollary B.2 that

$$\begin{aligned} \nabla_{\theta_n} (\tilde{\psi}_n \circ \mathcal{Z}_n) &= \beta^{-1}(d_{\mathfrak{m}_n(\theta_n)}((\tilde{\psi}_n \circ \mathcal{L}_{z_{n-1}}) \circ \exp) \circ \mathfrak{m}_n) \\ &= \mathfrak{m}_n^* \circ \alpha^{-1}(d_{\mathfrak{m}_n(\theta_n)}((\tilde{\psi}_n \circ \mathcal{L}_{z_{n-1}}) \circ \exp)) \\ &= \mathfrak{m}_n^* \circ \nabla_{\mathfrak{m}_n(\theta_n)}((\tilde{\psi}_n \circ \mathcal{L}_{z_{n-1}}) \circ \exp) \end{aligned}$$

Note that $\mathfrak{m}_n^*(\xi) = \sum_{j=1}^d \xi \otimes (\Delta x_n)^j \mathbf{e}_j = \xi \otimes \Delta x_n$ for any vector field ξ on $T\mathfrak{g}$. So

$$\nabla_{\theta_n} (\tilde{\psi}_n \circ \mathcal{Z}_n) = \nabla_{\mathfrak{m}_n(\theta_n)}((\tilde{\psi}_n \circ \mathcal{L}_{z_{n-1}}) \circ \exp) \otimes \Delta x_n.$$

Now, by Proposition 2.12 one has

$$\nabla_{\mathfrak{m}_n(\theta_n)}((\tilde{\psi}_n \circ \mathcal{L}_{z_{n-1}}) \circ \exp) = d_{\mathfrak{m}_n(\theta_n)^\top} \exp(\nabla_{\exp(\mathfrak{m}_n(\theta_n))} \tilde{\psi}_n \circ \mathcal{L}_{z_{n-1}}).$$

As before, since the left action on \mathfrak{g} corresponds to matrix multiplication, from the definition of \mathfrak{m}_n we may deduce that

$$\nabla_{\theta_n} (\tilde{\psi}_n \circ \mathcal{Z}_n) = d_{\mathfrak{m}_n(\theta_n)^\top} \exp(\nabla_{z_n} \tilde{\psi}_n \cdot z_{n-1}) \otimes \Delta x_n.$$

This completes the proof. \square

Our implementation of the development layer can be generalised to any adequate matrix Lie algebras via the map Proj in the Eq. (8). For example, we use a projection map for $\mathfrak{so}(m, \mathbb{R})$ as follows:

$$\text{Proj} : \mathfrak{gl}(m, \mathbb{R}) \longrightarrow \mathfrak{so}(m, \mathbb{R}), \quad M \longmapsto \frac{M - M^\top}{2}.$$

The corresponding Lie groups used in our implementation include the special orthogonal, unitary, real symplectic, and special Euclidean groups, as well as the group of orientation-preserving isometries of the hyperbolic space. We adapt <https://github.com/Lezcano/exprNN> for the PyTorch implementation of matrix exponential and its differential in Al-Mohy and Higham [2009, 2010]. In addition, we apply a scaling and square trick for computing the matrix exponential as in Higham [2005] to facilitate stabilisation of our model optimisation.

C Experimental Details

C.1 General Remarks

Optimizer All experiments used the ADAM optimiser as in Kingma and Ba [2014]. Learning rates and batch sizes vary along experiments and models. The learning rate in certain experiments may be applied with a constant exponential decay rate, and the training process is terminated when the metric failed to improve for some large number of epochs. See individual sections for details. We saved model checkpoints after every epoch whenever the validation set performance (the performance metric varies from experiment to experiment) gets improved and loaded the best performing model for evaluation on test set.

Architectures In our numerical experiments, we consider the development models (DEVs) and the hybrid model (LSTM+DEVs) by stacking the LSTM with the development layer together. To benchmark our development-based models, we use the signature model and the LSTM model as two baselines.

For the Speech Commands and Character Trajectories experiments, all the above mentioned models (DEVs, LSTM+DEVs, Signature, and LSTM) all include a linear output layer to predict the estimated probability of each class. For a fair comparison, we keep the total number of parameters across different models comparable and then compare the model performance in terms of accuracy and training stability.

Similarly, we also keep the model complexity of the baseline LSTM and our proposed hybrid model (LSTM+DEVSE(2)) comparable in the N -body simulation task. See the specific architecture of each individual model for those three datasets in Appendix C.2, Appendix C.3 and Appendix C.4 respectively.

Hyperparameters tuning Once our model architecture are fixed for fair comparison, our hyperparameter tuning mainly focused on the learning rate and batch size. Specifically, the learning rate is first set at 0.003 and reducing it until the good performance is achieved. And then we search the batch size with a grid of [32, 64, 128]. The decay factor of the learning rate was also applied to certain models if severe overfitting is observed on the validation set. Throughout the experiments, we notice that the hyperparameters have minimal affect on the development network model, whereas the RNN based models are very sensitive the hyperparameters.

Loss We used cross-entropy loss applied to the softmax function of the output of the model for the multi-classes classification problem. We used mean squared error loss for the regression problem in the N -Body simulation.

Computing infrastructure All experiments were run on five Quadro RTX 8000 GPUs. We ran all models with PyTorch 1.9.1 Paszke et al. [2019] and performed hyperparameter tuning with Wandb Biewald [2020].

Codes The code for reproducing all experiments can be found in <https://github.com/PDevNet/DevNet>

C.2 Speech Commands

We follow the exact data generating procedure in Kidger et al. [2020] and took a 70%/15%/15% train/validation/test split.

The batch size used was 128 for every model. Dev(SO), LSTM+Dev(SO) and signature model used a constant learning rate of 0.001 throughout the training. LSTM was trained with learning rate 0.001, with exponential decay rate of 0.997. If the validation accuracy stops improving for 50 epochs, we terminate the training process. The maximum training epochs is set to be 150.

Signature We apply the signature transform up to depth 3 on the input, which converts the input time series to a vector of size 8420 before passing to a output linear layer. The model has 84210 parameters in total.

LSTM The input of the model is passed to a single layer of LSTM (135 hidden units). The output of the LSTM (last time step) is passed to a output linear layer. It has 86140 parameters in total.

DEV(SO) The input of the model is passed to the special orthogonal development lyear (54 by 54 matrix hidden units). Then the output of the development (final time step) is passed to a final linear output layer. It has 87490 parameters in total.

LSTM-DEV(SO) The input of the model is passed to a single LSTM layer (56 hidden units). Then we pass the output of the LSTM (full sequence) to the special orthogonal development layer (32 by 32 matrix hidden units). Then the output of the development (final time step) is passed to a final linear output layer. It has 85066 parameters in total.

C.3 Character Trajectories

We followed the approach by Kidger et al. [2020], where we combined the train/test split of the original dataset and then took a 70%/15%/15% train/validation/test split.

The batch size used was 32 for every model. Dev(SO), LSTM+Dev(SO) and signature model used a constant learning rate of 0.001 throughout the training. LSTM was trained with a learning rate of 0.003, with an exponential decay rate of 0.997. If the validation accuracy stops improving for 50 epochs, we terminate the training process. The maximum training epochs is set to be 150.

Signature We apply the signature transform up to depth 4 on the input, which converts the input time series to a vector of size 340, then it is passed to a linear output layer. The model has 6820 parameters in total.

LSTM The input of the model is passed to a single layer of LSTM (40 hidden units). The output of the LSTM (last time step) is passed to a linear output layer. The model has 8180 parameters in total.

DEV(SO) The model’s input is passed to the special orthogonal development layer (20 by 20 matrix hidden units). Then the output of the development (final time step) is passed to a final linear output layer. The model has 7760 parameters in total.

LSTM-DEV(SO) The model’s input is passed to a single LSTM layer(14 hidden units). Then we pass the output of the LSTM (full sequence) to the special orthogonal development layer (14 by 14 matrix hidden units). Then the output of the development (final time step) is passed to a final linear output layer. The model has 8084 parameters in total.

C.4 N -body simulations

We followed Kipf et al. [2018] to simulate 2-dimensional trajectories of the five charged, interacting particles. The particles carry positive and negative charges, sampled with uniform probabilities, interacting according to the relative location and charges. We simulated 1000 training trajectories, 500 validation trajectories and 1000 test trajectories, each having 5000 time steps. Instead of inferring the dynamics of the complete trajectories as in Kipf et al. [2018], we consider it a regression problem with sequential input: the input data is a sequence of locations and velocities in the past 500 time steps (downsampled to the length of 50). The output data is the particle’s positions in the future k time steps for $k \in \{100, 300, 500\}$.

More specifically, let $(x_t^{(i)}, v_t^{(i)})$ denote the 2D location and velocity of the i^{th} particle at time t . The input and output of the regression problem are $\mathbf{x}_t = \left(\left((x_s^{(i)}, v_s^{(i)}) \right)_{s=t-500}^t \right)_{i=1}^5$ and $(x_{t+k}^{(i)})_{i=1}^5$, respectively.

In the 2-D space, the coordinate transform is described by the special Euclidean group $SE(2)$, which consists of composition of rotations and translations:

$$\begin{pmatrix} x' \\ y' \\ 1 \end{pmatrix} = T \begin{pmatrix} x \\ y \\ 1 \end{pmatrix} := \begin{pmatrix} R & t_x \\ 0 & 0 & 1 \end{pmatrix} \begin{pmatrix} x \\ y \\ 1 \end{pmatrix}, \quad (11)$$

where $T \in SE(2)$ and R is a 2-D rotation matrix.

The proposed LSTM+DEV(SE(2)) network architecture models the transformation map from $x_t^{(i)}$ to $x_{t+k}^{(i)}$, and hence predicts the future location by multiplying the output of the development layer with $x_t^{(i)}$. The model weights of each development layer to predict the i^{th} particle could be different.

The other three baselines include (1) the current location x_t (static estimator, assuming no further movements of the particle); and (2) the LSTM (3) To model the transformation map with the SO(2) development layer.

All models are trained with a learning rate of 0.001 with a 0.997 exponential decay rate. The batch size used was 128 for every model. The training was terminated if the validation MSE stopped lowering for 50 epochs. The maximum number of epochs was set to be 200.

For all models, we passed the input through two dense layers (16 hidden units), followed by a single LSTM layer (32 hidden units).

LSTM For the LSTM model, we pass the LSTM output (last time step) through one dense layer (32 hidden units) and a single linear output layer.

LSTM+DEV(SE(2)) we pass the LSTM output (full sequence) to the five independent SE(2) development layers (each has 3 by 3 matrix hidden units). The output of each independent development layer (final time step) is a Lie group element in SE(2). We apply the learned SE(2) element to the last observed location of each particle to estimate the future locations of the five particles, according to Equation (11).

LSTM+DEV(SO(2)) we pass the LSTM output (full sequence) to the five independent SO(2) development layers (each has 2 by 2 matrix hidden units). The output of each independent development layer (final time step) is a Lie group element in SO(2). We multiply the learned SO(2) element with the last observed location of each particle to estimate the future locations of the five particles.

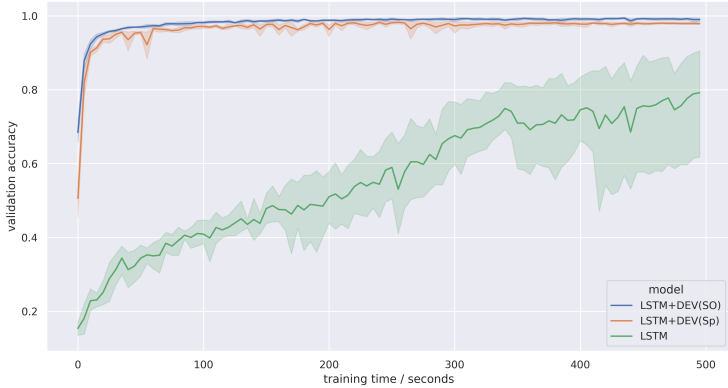
D Supplementary numerical results

We provide the supplementary numerical results on speech Commands dataset (Table 4) and Character Trajectory Dataset (Figure 6) in this subsection.

Table 4: Test accuracies of the linear model on development and signature baselines on Speech Commands dataset.

SIGNATURE		
DEPTH (<i>n</i>)	TEST ACCURACY	# FEATURE
1	12.3%	20
2	75.4%	420
3	85.7%	8420
4	88.9%	168420
DEVELOPMENT (DEV)		
ORDER (<i>m</i>)	TEST ACCURACY	# FEATURE
5	70.5%	25
10	81.3%	100
20	84.6%	400
30	86.2%	900
50	87.5%	2500
100	89.0 %	10000

Figure 6: Validation accuracy over the entire training period on Character Trajectories dataset. The average curve with its standard deviation indicated by the shaded area is computed over 5 runs.



References

- A. H. Al-Mohy and N. J. Higham. Computing the Fréchet derivative of the matrix exponential, with an application to condition number estimation. *SIAM Journal on Matrix Analysis and Applications*, 30(4):1639–1657, 2009.
- A. H. Al-Mohy and N. J. Higham. A new scaling and squaring algorithm for the matrix exponential. *SIAM Journal on Matrix Analysis and Applications*, 31(3):970–989, 2010.
- M. Arjovsky, A. Shah, and Y. Bengio. Unitary evolution recurrent neural networks. In *International Conference on Machine Learning*, pages 1120–1128, 2016.
- I. P. Arribas, G. M. Goodwin, J. R. Geddes, T. Lyons, and K. E. Saunders. A signature-based machine learning model for distinguishing bipolar disorder and borderline personality disorder. *Translational psychiatry*, 8(1):1–7, 2018.
- A. Bagnall, H. A. Dau, J. Lines, M. Flynn, J. Large, A. Bostrom, P. Southam, and E. Keogh. The UEA multivariate time series classification archive, 2018. *arXiv preprint arXiv:1811.00075*, 2018.
- S. Bai, J. Z. Kolter, and V. Koltun. An empirical evaluation of generic convolutional and recurrent networks for sequence modeling. *arXiv preprint arXiv:1803.01271*, 2018.
- Y. Bengio, P. Simard, and P. Frasconi. Learning long-term dependencies with gradient descent is difficult. *IEEE transactions on neural networks*, 5(2):157–166, 1994.
- L. Biewald. Experiment tracking with weights and biases, 2020. URL <https://www.wandb.com/>. Software available from wandb.com.
- H. Boedihardjo and X. Geng. $SL_2(\mathbb{R})$ -developments and Signature Asymptotics for Planar Paths with Bounded Variation. *arXiv preprint arXiv:2009.13082*, 2020.
- H. Boedihardjo, J. Diehl, M. Mezzarobba, and H. Ni. The expected signature of brownian motion stopped on the boundary of a circle has finite radius of convergence. *Bulletin of the London Mathematical Society*, 53(1):285–299, 2021.
- R. T. Chen, Y. Rubanova, J. Bettencourt, and D. Duvenaud. Neural ordinary differential equations. In *Proceedings of the 32nd International Conference on Neural Information Processing Systems*, pages 6572–6583, 2018.
- I. Chevyrev and A. Kormilitzin. A primer on the signature method in machine learning. *arXiv preprint arXiv:1603.03788*, 2016.
- I. Chevyrev and T. Lyons. Characteristic functions of measures on geometric rough paths. *The Annals of Probability*, 44(6):4049–4082, 2016.
- K. Cho, B. Van Merriënboer, D. Bahdanau, and Y. Bengio. On the properties of neural machine translation: Encoder-decoder approaches. *arXiv preprint arXiv:1409.1259*, 2014.
- E. De Brouwer, J. Simm, A. Arany, and Y. Moreau. GRU-ODE-Bayes: Continuous modeling of sporadically-observed time series. In *Advances in Neural Information Processing Systems 32*, 2019.
- B. K. Driver. A primer on Riemannian geometry and stochastic analysis on path spaces. *University of California, San Diego*, 1995.
- F. B. Fuchs, D. E. Worrall, V. Fischer, and M. Welling. SE(3)-transformers: 3d roto-translation equivariant attention networks. *arXiv preprint arXiv:2006.10503*, 2020.
- B. Hambly and T. Lyons. Uniqueness for the signature of a path of bounded variation and the reduced path group. *Annals of Mathematics*, pages 109–167, 2010.
- N. J. Higham. The scaling and squaring method for the matrix exponential revisited. *SIAM Journal on Matrix Analysis and Applications*, 26(4):1179–1193, 2005.
- S. Hochreiter and J. Schmidhuber. Long short-term memory. *Neural computation*, 9(8):1735–1780, 1997.
- P. Kidger, P. Bonnier, I. Perez Arribas, C. Salvi, and T. Lyons. Deep signature transforms. *Advances in Neural Information Processing Systems*, 32, 2019.
- P. Kidger, J. Morrill, J. Foster, and T. Lyons. Neural controlled differential equations for irregular time series. *Thirty-fourth Conference on Neural Information Processing Systems*, 2020.
- D. P. Kingma and J. Ba. Adam: A method for stochastic optimization. *arXiv preprint arXiv:1412.6980*, 2014.
- T. Kipf, E. Fetaya, K.-C. Wang, M. Welling, and R. Zemel. Neural relational inference for interacting systems. In *International Conference on Machine Learning*, pages 2688–2697. PMLR, 2018.
- D. Levin, T. Lyons, and H. Ni. Learning from the past, predicting the statistics for the future, learning an evolving system. *arXiv preprint arXiv:1309.0260*, 2013.

- M. Lezcano-Casado. Trivializations for gradient-based optimization on manifolds. *Advances in Neural Information Processing Systems*, 32:9157–9168, 2019.
- M. Lezcano-Casado and D. Martínez-Rubio. Cheap orthogonal constraints in neural networks: A simple parametrization of the orthogonal and unitary group. In *International Conference on Machine Learning*, pages 3794–3803. PMLR, 2019.
- X. Liu, S. Si, Q. Cao, S. Kumar, and C.-J. Hsieh. Neural SDE: Stabilizing neural ODE networks with stochastic noise. *arXiv preprint arXiv:1906.02355*, 2019.
- T. Lyons. Rough paths, signatures and the modelling of functions on streams. *the Proceedings of the International Congress of Mathematicians 2014, Korea*, 2014.
- T. Lyons and W. Xu. Hyperbolic development and inversion of signature. *Journal of Functional Analysis*, 272(7): 2933–2955, 2017.
- T. J. Lyons, M. Caruana, and T. Lévy. *Differential equations driven by rough paths*. Springer, 2007.
- J. Morrill, A. Kormilitzin, A. Nevado-Holgado, S. Swaminathan, S. Howison, and T. Lyons. The signature-based model for early detection of sepsis from electronic health records in the intensive care unit. In *2019 Computing in Cardiology (CinC)*, pages Page–1. IEEE, 2019.
- J. Morrill, C. Salvi, P. Kidger, and J. Foster. Neural rough differential equations for long time series. In *International Conference on Machine Learning*, pages 7829–7838. PMLR, 2021.
- A. Paszke, S. Gross, F. Massa, A. Lerer, J. Bradbury, G. Chanan, T. Killeen, Z. Lin, N. Gimelshein, L. Antiga, A. Desmaison, A. Kopf, E. Yang, Z. DeVito, M. Raison, A. Tejani, S. Chilamkurthy, B. Steiner, L. Fang, J. Bai, and S. Chintala. PyTorch: An Imperative Style, High-Performance Deep Learning Library. In *Advances in Neural Information Processing Systems 32*, pages 8024–8035. Curran Associates, Inc., 2019.
- D. W. Romero, R.-J. Brintjes, J. M. Tomczak, E. J. Bekkers, M. Hoogendoorn, and J. C. van Gemert. Flexconv: Continuous kernel convolutions with differentiable kernel sizes. *arXiv preprint arXiv:2110.08059*, 2021.
- W. Rossmann. *Lie Groups: An Introduction Through Linear Groups*. Oxford graduate texts in mathematics; 5. Oxford University Press, 2002. ISBN 0198596839.
- Y. Rubanova, R. T. Chen, and D. Duvenaud. Latent ODEs for irregularly-sampled time series. In *Proceedings of the 33rd International Conference on Neural Information Processing Systems*, pages 5320–5330, 2019.
- N. Thomas, T. Smidt, S. Kearnes, L. Yang, L. Li, K. Kohlhoff, and P. Riley. Tensor field networks: Rotation-and translation-equivariant neural networks for 3d point clouds. *arXiv preprint arXiv:1802.08219*, 2018.
- P. Warden. Speech commands: A dataset for limited-vocabulary speech recognition. *arXiv preprint arXiv:1804.03209*, 2018.
- Z. Xie, Z. Sun, L. Jin, H. Ni, and T. Lyons. Learning spatial-semantic context with fully convolutional recurrent network for online handwritten chinese text recognition. *IEEE transactions on pattern analysis and machine intelligence*, 40(8):1903–1917, 2017.
- B. Zheng, N. Vijaykumar, and G. Pekhimenko. Echo: Compiler-based GPU memory footprint reduction for LSTM RNN training. In *2020 ACM/IEEE 47th Annual International Symposium on Computer Architecture (ISCA)*, pages 1089–1102. IEEE, 2020.